




## Article

# Sapozhnikovite, $\text{Na}_8(\text{Al}_6\text{Si}_6\text{O}_{24})(\text{HS})_2$ , a new sodalite-group mineral from the Lovozero alkaline massif, Kola Peninsula

Nikita V. Chukanov<sup>1,2\*</sup>, Natalia V. Zubkova<sup>2</sup>, Igor V. Pekov<sup>2,3</sup>, Roman Yu. Shendrik<sup>4</sup>, Dmitry A. Varlamov<sup>5</sup> , Marina F. Vigasina<sup>2</sup>, Dmitry I. Belakovskiy<sup>6</sup>, Sergey N. Britvin<sup>7</sup>, Vasilii O. Yapaskurt<sup>2</sup> and Dmitry Yu. Pushcharovskiy<sup>2</sup>

<sup>1</sup>Institute of Problems of Chemical Physics, Russian Academy of Sciences, Chernogolovka, Moscow region, 142432 Russia; <sup>2</sup>Faculty of Geology, Moscow State University, Vorobiev Gory, 119991 Moscow, Russia; <sup>3</sup>Vernadsky Institute of Geochemistry and Analytical Chemistry, Russian Academy of Sciences, Kosygina str. 19, 119991 Moscow, Russia; <sup>4</sup>Vinogradov Institute of Geochemistry, Siberian Branch of Russian Academy of Sciences, 1a Favorskii St., Irkutsk, 664033, Russia; <sup>5</sup>Institute of Experimental Mineralogy, Russian Academy of Sciences, Chernogolovka, 142432 Russia; <sup>6</sup>Fersman Mineralogical Museum of the Russian Academy of Sciences, Leninsky Prospekt 18-2, 119071 Moscow, Russia; and <sup>7</sup>Department of Crystallography, St Petersburg State University, Universitetskaya Nab. 7/9, 199034 St Petersburg, Russia

### Abstract

The new sodalite-group mineral sapozhnikovite, ideally  $\text{Na}_8(\text{Al}_6\text{Si}_6\text{O}_{24})(\text{HS})_2$ , was discovered in a hydrothermally altered urtite-like rock at Karnasurt Mountain, Lovozero alkaline massif, Kola Peninsula, Russia. The associated minerals are nepheline, aegirine, potassic feldspar, albite, kyanoxalite, natrolite, fluorapatite, fluorcaphite, lomonosovite (partially or completely altered to murmanite) and loparite-(Ce). Sapozhnikovite forms isolated colourless to pale greyish anhedral equant grains up to 5 mm across. The streak is white and the lustre is vitreous. Strong orange fluorescence under longwave UV radiation ( $\lambda = 330$  nm) and weak yellow-orange fluorescence under shortwave UV radiation ( $\lambda = 245$  nm) is observed. Sapozhnikovite is brittle, with a Mohs hardness of 5½. Cleavage is imperfect on (110). Density measured by flotation in heavy liquids is equal to 2.25(1) g·cm<sup>-3</sup>. The calculated density is 2.255 g·cm<sup>-3</sup>. Sapozhnikovite is characterised by infrared, Raman, electron spin resonance, NIR-Vis-UV absorption, and photoluminescence spectroscopy. The chemical composition is (wt.%, electron microprobe, H<sub>2</sub>O determined by gas chromatography of ignition products): Na<sub>2</sub>O 25.05, Al<sub>2</sub>O<sub>3</sub> 32.44, SiO<sub>2</sub> 37.58, HS 4.33, Cl 2.22, H<sub>2</sub>O 0.30, -O≡(Cl,HS) -1.55, total 100.37. The empirical formula is  $\text{Na}_{7.73}\text{Al}_{6.08}\text{Si}_{5.97}\text{O}_{24}(\text{HS})_{1.25}\text{Cl}_{0.60}\cdot 0.16\text{H}_2\text{O}$ . The crystal structure was determined using single-crystal X-ray diffraction data and refined to  $R_1 = 1.62\%$ . Sapozhnikovite is cubic,  $P43n$ , with  $a = 8.9146(1)$  Å,  $V = 708.45(2)$  Å<sup>3</sup> and  $Z = 1$ . The new mineral is isostructural with sodalite. The strongest lines of the powder X-ray diffraction pattern [ $d$ , Å ( $I$ , %) ( $hkl$ )] are: 6.30 (37) (110), 3.638 (100) (211), 2.821 (14) (310), 2.572 (18) (222), 2.382 (16) (321) and 2.101 (29) (411). The mineral is named in honour of the Russian mineralogist and crystallographer Dr. Anatoly Nikolaevich Sapozhnikov (b. 1946).

**Keywords:** sapozhnikovite, new mineral, sodalite group, crystal structure, IR spectroscopy, Raman spectroscopy, electron spin resonance, NIR-Vis-UV spectroscopy, photoluminescence, Lovozero alkaline massif, Kola Peninsula

(Received 13 September 2021; accepted 1 December 2021; Accepted Manuscript published online: 10 December 2021; Associate Editor: Charles A Geiger)

### Introduction

The SOD-type framework in sodalite-group minerals and related compounds can be described as consisting of three kinds of stacked layers (A, B and C) of Al- and Si-centred tetrahedra, in the sequence (ABC)<sub>∞</sub> (Bonaccorsi and Merlino, 2005; see also Database of Zeolite Structures, <http://www.iza-structure.org/databases/>). The layers contain six-membered rings of Si- and Al-centred tetrahedra which are ordered in most aluminosilicate sodalite-group minerals. The distinguishing structural feature of sodalite-type compounds is a system of intersecting channels

consisting of sodalite cages. The species-defining extra-framework components in sodalite-group minerals include different cations ( $\text{Na}^+$ ,  $[\text{N}(\text{CH}_3)_4]^+$ ,  $\text{Ca}^{2+}$ ,  $\text{Mn}^{2+}$ ,  $\text{Fe}^{2+}$  and  $\text{Zn}^{2+}$ ), anions ( $\text{Cl}^-$ ,  $\text{F}^-$ ,  $\text{OH}^-$ ,  $\text{HS}^-$ ,  $\text{S}^{2-}$ ,  $\text{SO}_4^{2-}$  and radical anion  $\text{S}_3^{\cdot-}$ ) and neutral molecules ( $\text{H}_2\text{O}$ ) (Chukanov *et al.*, 2021a) (‘·’ denotes unpaired electron). Other extra-framework species ( $\text{K}^+$ ,  $\text{S}_2^{\cdot-}$ ,  $\text{SO}_4^{2-}$ ,  $\text{S}_3$ ,  $\text{S}_4$ ,  $\text{S}_6$ ,  $\text{CO}_2$  and  $\text{COS}$ ) occur in subordinate amounts and can be identified based on a multianalytical approach involving different spectroscopic methods (Chukanov *et al.*, 2020a, 2020b; Sapozhnikov *et al.*, 2021).

Sodalite-group minerals are widespread in different kinds of alkaline igneous and metasomatic rocks and sometimes play a rock-forming role. Chemical diversity of natural SOD-type compounds is mainly due to geochemical factors (Chukanov *et al.*, 2021a).

The new mineral sapozhnikovite,  $\text{Na}_8(\text{Al}_6\text{Si}_6\text{O}_{24})(\text{HS})_2$ , described in this paper is the first member of the sodalite group containing the  $\text{HS}^-$  anion as a species-defining component. The

\*Author for correspondence: Nikita V. Chukanov, Email: [chukanov@icp.ac.ru](mailto:chukanov@icp.ac.ru)

Cite this article: Chukanov N.V., Zubkova N.V., Pekov I.V., Shendrik R.Yu., Varlamov D.A., Vigasina M.F., Belakovskiy D.I., Britvin S.N., Yapaskurt V.O., Pushcharovskiy D.Yu. (2022) Sapozhnikovite,  $\text{Na}_8(\text{Al}_6\text{Si}_6\text{O}_{24})(\text{HS})_2$ , a new sodalite-group mineral from the Lovozero alkaline massif, Kola Peninsula. *Mineralogical Magazine* 86, 49–59. <https://doi.org/10.1180/mgm.2021.94>

mineral is named in honour of the outstanding Russian mineralogist and crystallographer, Senior Researcher of the Vinogradov Institute of Geochemistry, Siberian Branch of Russian Academy of Sciences (Irkutsk), Dr. Anatoly Nikolaevich Sapozhnikov (b. 1946). Dr. Sapozhnikov is the author of numerous scientific publications, a major part of which is related to structural chemistry of cancrinite- and sodalite-group minerals. Dr. Sapozhnikov is a senior author or co-author of a number of papers documenting the discoveries of a dozen of new mineral species including four minerals belonging to the cancrinite and sodalite groups (bystrite, tounkite, vladimirivanovite and sulfhydrylbystrite).

The new mineral and its name (symbol Spz) have been approved by the International Mineralogical Association's Commission on New Minerals, Nomenclature and Classification (IMA2021-030, Chukanov, 2021b). The holotype specimen is deposited in the collection of the Fersman Mineralogical Museum of the Russian Academy of Sciences, Moscow, Russia with the registration number 5665/1.

### Experimental methods and data processing

In order to obtain infrared (IR) absorption spectra of sapozhnikovite and other sodalite-group minerals (used for comparison), powdered samples were mixed with anhydrous KBr, pelletised, and analysed using an ALPHA FTIR spectrometer (Bruker Optics) at a resolution of  $4\text{ cm}^{-1}$ . Sixteen scans were collected for each spectrum. The IR spectrum of a pellet of pure KBr was used as a reference.

Raman spectra of randomly oriented grains of sapozhnikovite and sodalite-group minerals used for comparison were obtained using an EnSpectr R532 spectrometer based on an OLYMPUS CX 41 microscope coupled with a diode laser ( $\lambda = 532\text{ nm}$ ) at room temperature. The spectra were recorded in the range from 100 to  $4000\text{ cm}^{-1}$  with a diffraction grating ( $1800\text{ gr mm}^{-1}$ ) and spectral resolution of  $\sim 6\text{ cm}^{-1}$ . The output power of the laser beam was in the range from 5 to 13 mW. The diameter of the focal spot on the sample was 5–10  $\mu\text{m}$ . The back-scattered Raman signal was collected with a 40 $\times$  objective; signal acquisition time for a single scan of the spectral range was 1 s, and the signal was averaged over 50 scans. Crystalline silicon was used as a standard.

Electron spin resonance (ESR) spectra were recorded using a RE-1306 X-band spectrometer (KBST, Smolensk, Russia) with a frequency of 9.358 GHz. Small randomly oriented crystals of sapozhnikovite were placed in a quartz test tube. The measurements were carried out at room temperature.

Diffuse-light near infrared (NIR), visible (Vis), and near ultraviolet (UV) absorption spectra of sapozhnikovite were measured at room temperature with a PerkinElmer Lambda 950 spectrophotometer (Perkin-Elmer, Shelton, CT, USA) in an integrating sphere. For measurements, the samples were placed in a quartz test tube, which is transparent in the range of 285–2000 nm ( $35,000\text{--}5000\text{ cm}^{-1}$ ). The light beam was completely concentrated on the sample. The photoluminescence spectra were measured with excitation by laser radiation with a wavelength of 405 nm ( $24,690\text{ cm}^{-1}$ ). The luminescence signal was recorded using a Hamamatsu H6780-04 photomodule (185–850 nm) operating in the photon counting regime equipped by a SDL-1 double grating monochromator (LOMO, St. Petersburg, Russia) with a diffraction grating of 600 lines per mm, at a spectral slit width of 0.05 nm. The measurements at 77 K were carried out in a flooded nitrogen cryostat; the sample was attached to a cryofinger and the

temperature was recorded using a type-K thermocouple. The excitation spectrum is normalised utilising the calibration curve obtained by means of a highly fluorescent rhodamine family dye Rhodamine-6G. The photoluminescence spectrum of sapozhnikovite was obtained at 77 K.

Electron microprobe analyses were obtained in WDS mode (20 kV and 10 nA; the electron beam was rastered to a  $5\text{ }\mu\text{m} \times 5\text{ }\mu\text{m}$  area to minimise damage to the mineral) and gave detectable contents of Na, Al, Si, O, Cl and S.

Gas chromatography of products of ignition in an oxygen stream at  $1200^\circ\text{C}$  was used to determine H, N and C.

Powder X-ray diffraction (XRD) data were collected using a Rigaku R-Axis Rapid II diffractometer (image plate),  $\text{CoK}\alpha$ , 40 kV, 15 mA, rotating anode with the microfocus optics, Debye-Scherrer geometry,  $d = 127.4\text{ mm}$  and exposure 15 min. The raw powder XRD data were collected using a program suite designed by Britvin *et al.* (2017). Calculated intensities were obtained using the *STOE WinXPOW v. 2.08* program suite based on the atomic coordinates and unit-cell parameters.

Single-crystal XRD studies were carried out using an Xcalibur S diffractometer equipped with a CCD detector ( $\text{MoK}\alpha$  radiation). The crystal structure study of sapozhnikovite was carried out on a crystal  $0.23\text{ mm} \times 0.31\text{ mm} \times 0.39\text{ mm}$  in size using an Xcalibur S single-crystal diffractometer equipped with a CCD detector. A full sphere of three-dimensional data was collected. Data reduction was performed using *CrysAlisPro* version 1.171.39.46 (Rigaku Oxford Diffraction, 2018). The data were corrected for Lorentz factor and polarisation effect. The crystal structure was refined using the *SHELX* software package (Sheldrick, 2015) to  $R = 0.0162$  for 334 unique reflections with  $I > 2\sigma(I)$  in the frame of the space group  $P4_3n$ . Crystal data, data collection information and structure refinement details for sapozhnikovite are given in Table 1.

## Results

### Occurrence, general appearance and physical properties

Sapozhnikovite occurs in a specific hydrothermally altered urtite-like rock at the northern slope of the Karnasurt Mountain located in the northern part of the Lovozero alkaline massif, Kola Peninsula, Russia. The associated minerals are nepheline, aegirine, potassic feldspar, albite, kyanoxalite, natrolite, fluorapatite, fluorcaphite, lomonosovite (partially or completely altered to murmanite) and loparite-(Ce). Sapozhnikovite is a rock-forming mineral in this rock, together with nepheline (typically  $> 60\text{ vol.}\%$ ), aegirine, alkali feldspars and kyanoxalite. The content of sapozhnikovite in the rock is up to 10–15 vol.%. Similar rocks from this region contain sodalite-group minerals with variable S:Cl ratios and belong to the sapozhnikovite–sodalite solid-solution series.

Sapozhnikovite occurs as isolated colourless to pale greyish anhedral equant grains up to 1 mm, rarely up to 5 mm across (Figs 1 to 3). The streak is white and the lustre is vitreous.

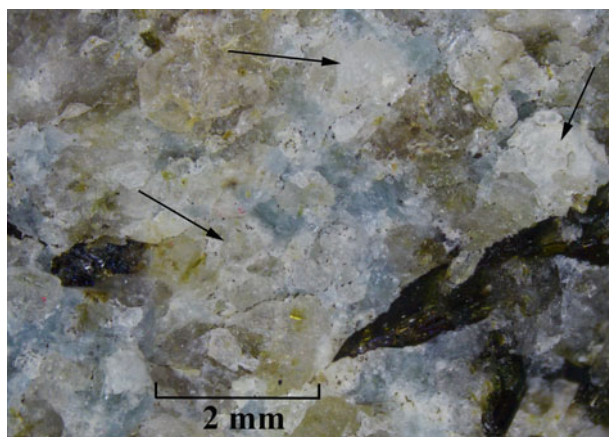
Intensive orange photoluminescence under longwave UV radiation ( $\lambda = 330\text{ nm}$ ) and weak yellow-orange photoluminescence under shortwave UV radiation ( $\lambda = 245\text{ nm}$ ) are observed. The photoluminescence is attributed to the presence of trace amounts of the  $\text{S}_2^-$  radical anion (see below for details).

Sapozhnikovite is brittle, with a Mohs hardness of  $5\frac{1}{2}$ . Cleavage is imperfect on (110). The fracture is uneven. Density measured by flotation in heavy liquids (bromoform + heptane) is equal to  $2.25(1)\text{ g}\cdot\text{cm}^{-3}$ . Density calculated using the empirical

**Table 1.** Crystal data, data collection information and structure refinement details for sapozhnikovite.

Crystal data	
Formula	$\text{Na}_{7.82}(\text{Si}_6\text{Al}_6\text{O}_{24})[(\text{HS})_{1.22}\text{Cl}_{0.60}(\text{H}_2\text{O})_{0.16}]$
Formula weight	956.23
Temperature (K)	293(2)
Radiation and wavelength (Å)	MoK $\alpha$ ; 0.71073
Crystal system, space group, Z	Cubic, $P43n$ , 1
Unit-cell dimensions (Å)	$a = 8.9146(1)$
$V$ (Å <sup>3</sup> )	708.45(2)
Absorption coefficient $\mu$ (mm <sup>-1</sup> )	0.836
$F_{000}$	471
Data collection	
Crystal size (mm)	0.23 × 0.31 × 0.39
Diffractometer	Xcalibur S CCD
Absorption correction	Multi-scan
$\theta$ range for data collection (°)	3.232–30.801
Index ranges	$-12 \leq h \leq 12$ , $-12 \leq k \leq 12$ , $-11 \leq l \leq 12$
Reflections collected	10,280
Independent reflections	374 ( $R_{\text{int}} = 0.0323$ )
Independent reflections with $I > 2\sigma(I)$	334
Refinement	
Refinement method	Full-matrix least-squares on $F^2$
Number of refined parameters	21
Final $R$ indices [ $I > 2\sigma(I)$ ]	$R_1 = 0.0162$ , $wR_2 = 0.0372^*$
$R$ indices (all data)	$R_1 = 0.0211$ , $wR_2 = 0.0413^*$
GoF	1.176
Largest diff. peak and hole (e <sup>-</sup> /Å <sup>3</sup> )	0.19 and -0.15

\*During the refinement, the occupancy of the site containing S, Cl and O atoms of water molecule was refined as S vs. O. The content of Cl was assumed based on chemical composition data and the refined number of electrons.

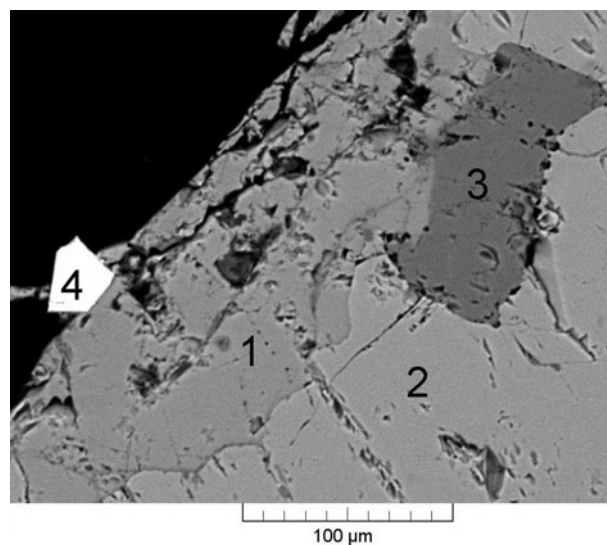
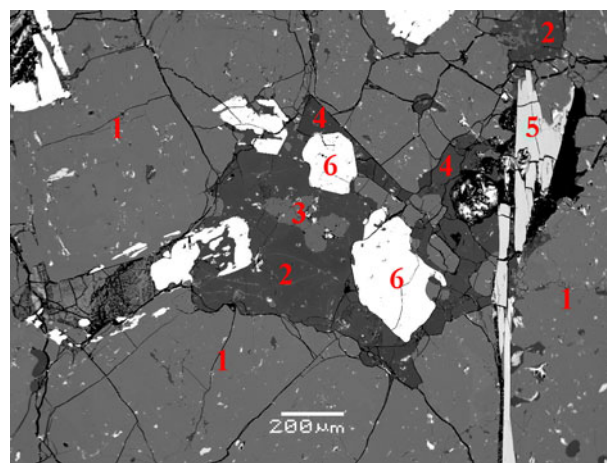
**Fig. 1.** Sapozhnikovite grains (indicated with arrows) in association with nepheline (pale greenish-grey), kyanoxalite (pale blue) and aegirine (black). Holotype specimen 5665/1.

formula and unit-cell volume refined from single-crystal XRD data is 2.255 g·cm<sup>-3</sup>.

The new mineral is optically isotropic, with  $n = 1.499(2)$  ( $\lambda = 589$  nm). Under the microscope, sapozhnikovite is colourless.

### Infrared spectroscopy

The assignment of absorption bands in the IR spectrum of sapozhnikovite (Fig. 4) is as follows. The band at 3520 cm<sup>-1</sup> corresponds to O–H stretching vibrations of H<sub>2</sub>O molecules in sodalite cages forming medium-strength hydrogen bonds (Chukanov, 2014; Chukanov and Chervonnyi, 2016; Nakamoto, 2008, 2009). The band at 2554 cm<sup>-1</sup> corresponds to stretching vibrations of the HS<sup>-</sup> anion (Sheppard, 1949; Bragin *et al.*, 1977). The band

**Fig. 2.** Sapozhnikovite (1) in association with nepheline (2), kyanoxalite (3) and aegirine (4). Back-scatter electron (BSE) image of a polished section. Holotype specimen 5665/1.**Fig. 3.** Mineral association including (1) nepheline, (2) kyanoxalite, (3) sapozhnikovite, (4) natrolite, (5) murmanite and (6) aegirine. BSE image of a polished section. Holotype specimen 5665/1.

at 1637 cm<sup>-1</sup> is due to bending vibrations of H<sub>2</sub>O molecules in sodalite cages (Chukanov 2014; Chukanov and Chervonnyi 2016; Nakamoto 2008, 2009).

The bands in the range 980–1080 cm<sup>-1</sup> correspond to stretching vibrations of the aluminosilicate framework, i.e. vibrations in which a major part of energy corresponds to changes of the covalent T–O bond lengths (T=Si and Al) (Chukanov and Chervonnyi, 2016). The bands at 660–740 cm<sup>-1</sup> correspond with mixed vibrations of the aluminosilicate framework involving changes of both T–O bond lengths and O–T–O angles. Below 500 cm<sup>-1</sup> bands are due to lattice modes involving soft T–O–T bending internal coordinates and libration vibrations of H<sub>2</sub>O molecules.

The intensity of S–H stretching vibrations, including the stretching band of the HS<sup>-</sup> anion, are very low (Sheppard, 1949; Bragin *et al.*, 1977; see Supplementary figure 1S). For this reason, Raman spectroscopy was used to confirm the presence of significant amounts of HS<sup>-</sup> in sapozhnikovite (see below).

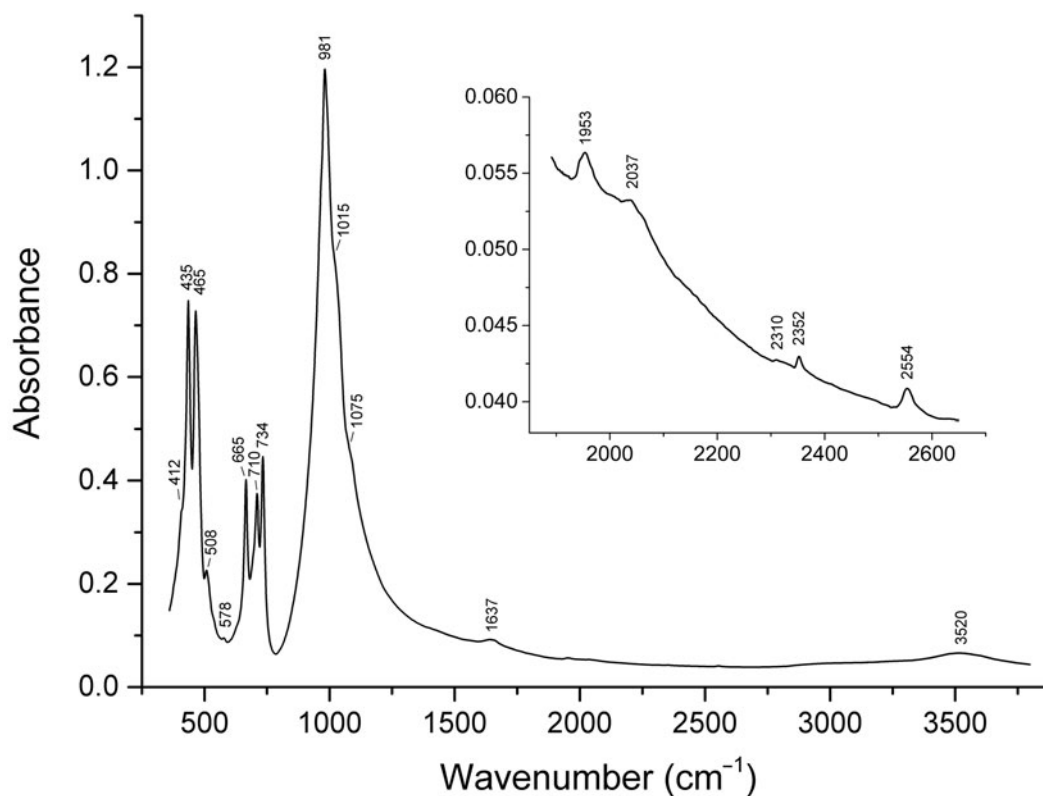


Fig. 4. Powder infrared absorption spectrum of sapozhnikovite.

The weak bands at  $2352$  and  $2037$   $\text{cm}^{-1}$  correspond to trace amounts of the extra-framework  $\text{CO}_2$  and  $\text{COS}$  neutral molecules, respectively (below 0.02 wt.% of each, as estimated from the band intensities: see Chukanov *et al.*, 2020a,2020b for the band assignment and the method of estimation). The weak bands at  $1953$  and  $578$   $\text{cm}^{-1}$  are assigned to overtones of stretching vibrations of the framework and vibrations involving  $\text{Na}^+$  cations, respectively (see Hettmann *et al.*, 2012).

Bands of sulfate groups in the IR spectra of sodalite-group minerals are observed as an absorption maximum in the range of  $1134$ – $1142$   $\text{cm}^{-1}$  [asymmetric stretching vibrations of  $\text{SO}_4^{2-}$ , the  $F_2(\nu_3)$  mode] and in the range of  $610$ – $630$   $\text{cm}^{-1}$  [bending vibrations of  $\text{SO}_4^{2-}$ , the  $F_2(\nu_4)$  mode] (Nakamoto 2008, 2009) (Supplementary figure 2S). These bands are absent in the IR spectra of both sapozhnikovite and S-free sodalite (Supplementary figure 2S).

Characteristic bands of  $\text{CO}_3^{2-}$  anions (in the range of  $1350$ – $1550$   $\text{cm}^{-1}$ ) are not observed in the IR spectrum of sapozhnikovite.

### Raman spectroscopy

The assignment of absorption bands in the Raman spectrum of sapozhnikovite (curve *a* in Fig. 5) is as follows. The strong band at  $2553$   $\text{cm}^{-1}$  corresponds to stretching vibrations of the  $\text{HS}^-$  anion (Bragin *et al.*, 1977). Bands in the range of  $970$ – $1070$   $\text{cm}^{-1}$  are assigned to stretching vibrations of the aluminosilicate framework, i.e. vibrations in which a major part of energy corresponds to changes of the covalent  $T$ – $\text{O}$  bond lengths (Hettmann *et al.*, 2012; see Supplementary figure 3S). The  $732$   $\text{cm}^{-1}$  band is due to mixed vibrations of the aluminosilicate framework involving changes of both  $T$ – $\text{O}$  bond lengths and  $\text{O}$ – $T$ – $\text{O}$  angles. The band at  $611$   $\text{cm}^{-1}$  is, presumably, an

overtone of the band at  $294$   $\text{cm}^{-1}$  corresponding to vibrations involving  $\text{Na}^+$  cations. Positive anharmonic shift is in agreement with this assignment.

The band at  $459$   $\text{cm}^{-1}$  corresponds to stretching vibrations of the  $[\text{ClNa}_4]$  cluster (Hettmann *et al.*, 2012; see Supplementary figure 3S) and  $417$   $\text{cm}^{-1}$ , presumably, is due to lattice modes involving soft  $T$ – $\text{O}$ – $T$  bending internal coordinates. Bands at  $260$  and  $294$   $\text{cm}^{-1}$  are due to bending vibrations of the  $[\text{ClNa}_4]$  cluster (Hettmann *et al.*, 2012; see Supplementary figure 3S).

The Raman spectrum of S-free sodalite (curve *b* in Fig. 5) is close to that of HS-sodalite in the range of  $200$ – $1200$   $\text{cm}^{-1}$  but does not contain the band of stretching vibrations of the  $\text{HS}^-$  anion.

The Raman spectra of sulfate-bearing sodalite-group minerals (including that of nosean: see curve *c* in Fig. 5) contain bands in the ranges of  $1135$ – $1140$ ,  $618$ – $625$  and  $436$ – $442$   $\text{cm}^{-1}$  corresponding to the  $F_2(\nu_3)$ ,  $F_2(\nu_4)$ , and  $E(\nu_2)$  modes of  $\text{SO}_4^{2-}$ , respectively. These bands are absent in the Raman spectra of sapozhnikovite and S-free sodalite.

In the Raman spectrum of lazurite (Supplementary figure 4S), another sodalite-group mineral containing sulfide sulfur, all observed bands correspond to the  $\text{S}_3^-$  radical anion which is a blue chromophore (Chukanov *et al.*, 2020b). These bands are also absent in the Raman spectrum of sapozhnikovite.

Bands of  $\text{CO}_3^{2-}$  are not observed in the Raman spectrum of sapozhnikovite.

### Electron spin resonance spectroscopy

In the ESR spectrum of sapozhnikovite, a broad intensive signal with  $g = 1.99$  and a poorly resolved structure is observed (Fig. 6).

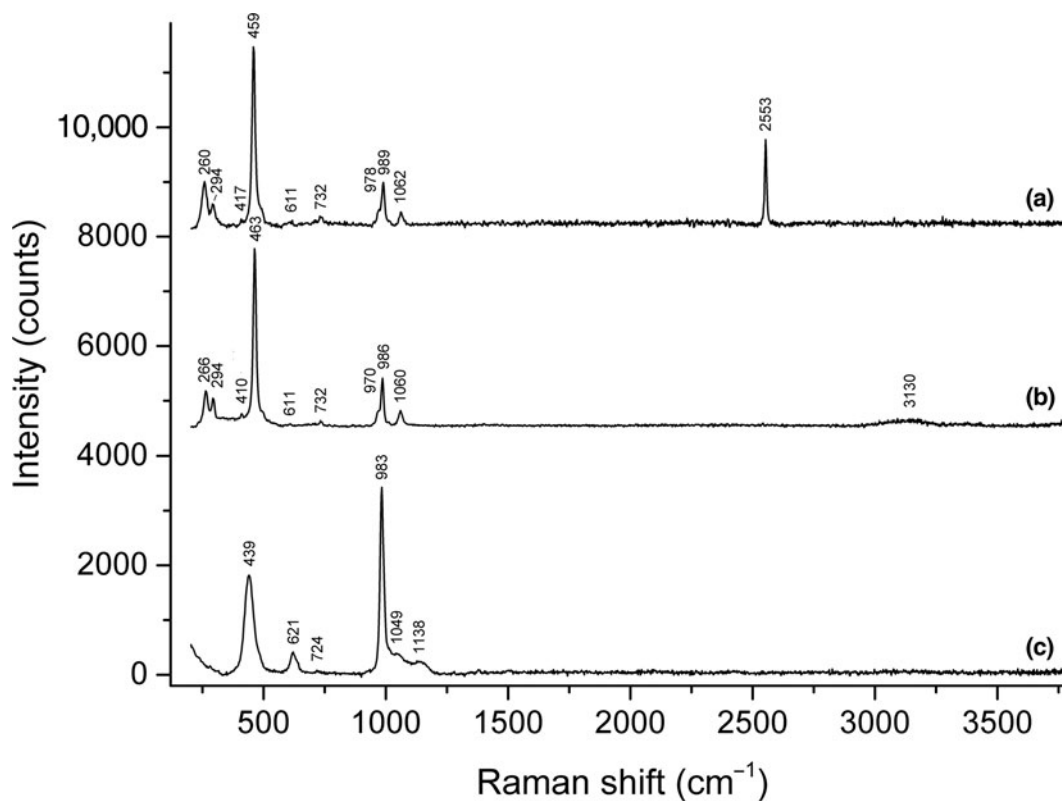


**Fig. 5.** Raman spectra of: (a) sapozhnikovite; (b) S-free sodalite from the Vishnevogorskiy syenite–miaskite complex; and (c) nosean from the Laach Lake volcano. The spectra are offset for comparison.

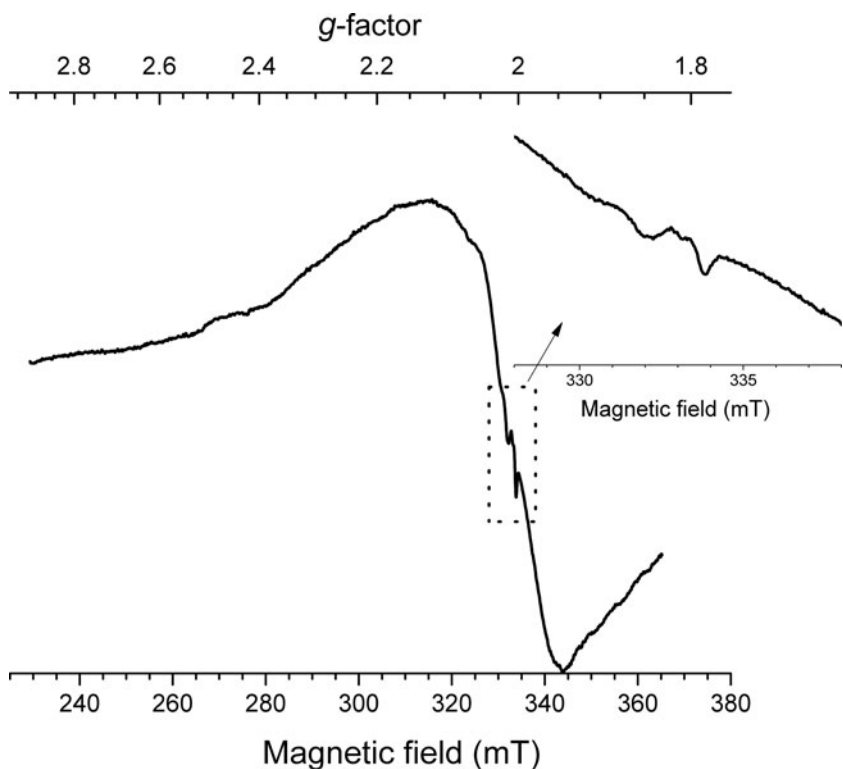


**Fig. 6.** Room-temperature first derivative ESR spectrum of sapozhnikovite.

In addition, very weak signals with  $g = 2.008$  and  $g = 2.001$  are detected (Fig. 6, inset). Assignment of these signals is detailed in the Discussion section below.

In order to estimate any possible content of  $S_2^{2-}$  in sapozhnikovite (suggested by the signals at  $g = 2.008$  and  $g = 2.001$ ) the intensity of the ESR signal was compared with the ESR spectrum of

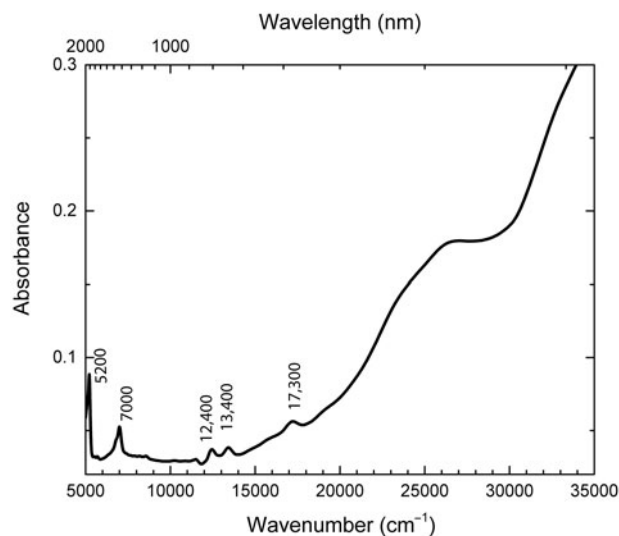


Fig. 7. NIR-Vis-UV absorption spectrum of sapozhnikovite.

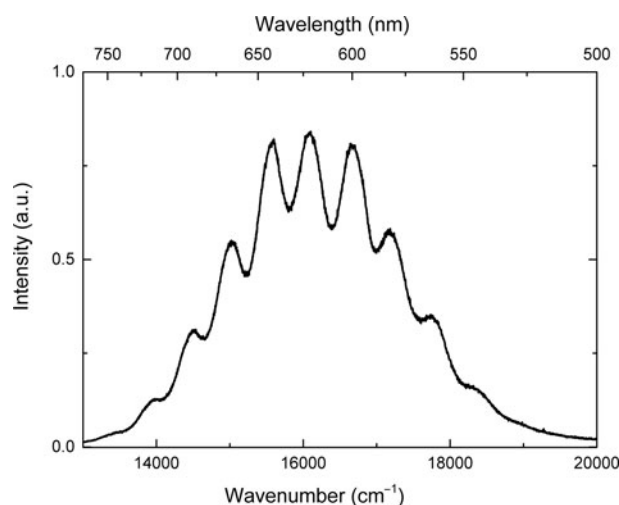


Fig. 8. Photoluminescence spectrum of sapozhnikovite excited by 405 nm (24,690  $\text{cm}^{-1}$ ) radiation at 77 K.

häüyne containing 0.06 wt.% of sulfide sulfur obtained under the same conditions (see Chukanov *et al.*, 2020b, Sample LSh). According to optical spectroscopy, ESR and Raman spectroscopy data, only a part of the sulfide sulfur in Sample LSh belongs to  $\text{S}_2^{2-}$ . The intensity of the  $\text{S}_2^{2-}$  signal in the ESR spectrum of sapozhnikovite is about 10 times weaker than the analogous signal of Sample LSh. Both signals are characterised by nearly the same relaxation time. According to these data, the content of  $\text{S}_2^{2-}$  in sapozhnikovite does not exceed 0.006 wt.%. Such low contents of  $\text{S}_2^{2-}$  cannot be detected by means of X-ray structural analysis.

#### Optical (NIR-Vis-UV) absorption spectroscopy

The diffuse optical absorption spectrum of sapozhnikovite in the near infrared (NIR), visible (Vis), and near ultraviolet (UV) ranges is given in Fig. 7. The bands at  $\sim 5200$  and  $\sim 7000$   $\text{cm}^{-1}$  correspond to the stretching and bending combination mode and overtone of O–H stretching mode of the extra-framework  $\text{H}_2\text{O}$  molecules, respectively. In addition, absorption bands at  $\sim 12,400$ ,  $\sim 13,400$  and  $\sim 17,300$   $\text{cm}^{-1}$  and a broad shoulder in the range of 23,000–28,000  $\text{cm}^{-1}$  are observed.

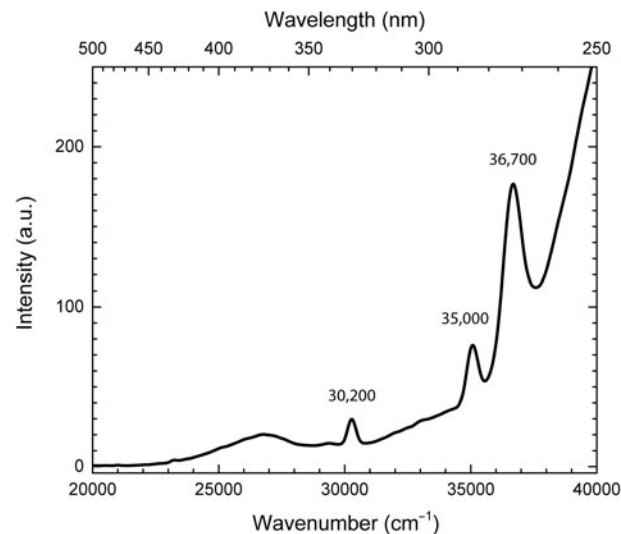


Fig. 9. Excitation spectrum of photoluminescence monitored at 625 nm (16,000  $\text{cm}^{-1}$ ) at 77 K.

#### Photoluminescence spectroscopy

The photoluminescence spectrum of sapozhnikovite with a maximum at 16,000  $\text{cm}^{-1}$  (Fig. 8) was obtained at 77 K. At this temperature, the vibrational structure of the spectrum is well-resolved with distance between satellites at  $\sim 536$   $\text{cm}^{-1}$ .

The excitation spectrum related to observed photoluminescence is given in Fig. 9. A broad band in the range of 23,000–28,000  $\text{cm}^{-1}$  and narrow bands with the maxima at  $\sim 30,200$ ,  $\sim 35,000$  and  $\sim 36,700$   $\text{cm}^{-1}$  are detected.

#### Chemical data

Five spot electron microprobe analyses were obtained for Na, Al, Si, S and Cl and a single gas chromatography analysis was obtained for H, C and N. Grains of sapozhnikovite are quite homogenous chemically (Fig. 10).

Analytical data are given in Table 2. The contents of other elements with atomic numbers higher than that of beryllium are below detection limits, in accordance with IR and Raman spectroscopy and gas chromatography data.

Direct determination of oxygen by electron microprobe (under conditions indicated above and using anorthite as a standard) resulted in 40.1 wt.% O. The content of oxygen calculated from the empirical formula is 39.8 wt.%. Taking into account the presence of trace amounts of extra-framework  $\text{CO}_2$  and  $\text{COS}$  molecules (below 0.02 wt.% of each, according to the IR spectroscopy data: see above), one can conclude that the calculated and measured contents of oxygen in sapozhnikovite are in a very good agreement. This confirms the absence of oxygen-bearing extra-framework anions ( $\text{SO}_4^{2-}$ ,  $\text{SO}_3^{2-}$ ,  $\text{CO}_3^{2-}$ , etc.) in sapozhnikovite.

The empirical formula based on 24 framework O atoms is  $\text{Na}_{7.73}\text{Al}_{6.08}\text{Si}_{5.97}\text{O}_{24}(\text{HS})_{1.25}\text{Cl}_{0.60}\cdot 0.16\text{H}_2\text{O}$ . The simplified formula is  $\text{Na}_8(\text{Al}_6\text{Si}_6\text{O}_{24})[(\text{HS}),\text{Cl},(\text{H}_2\text{O})]_2$ . The ideal formula of sapozhnikovite is  $\text{Na}_8(\text{Al}_6\text{Si}_6\text{O}_{24})(\text{HS})_2$ .

#### X-ray diffraction and crystal structure

Powder X-ray diffraction data of sapozhnikovite are listed in Table 3. The unit-cell parameters refined from the powder data are:  $a = 8.919(1)$  Å and  $V = 709.4(2)$  Å<sup>3</sup>.

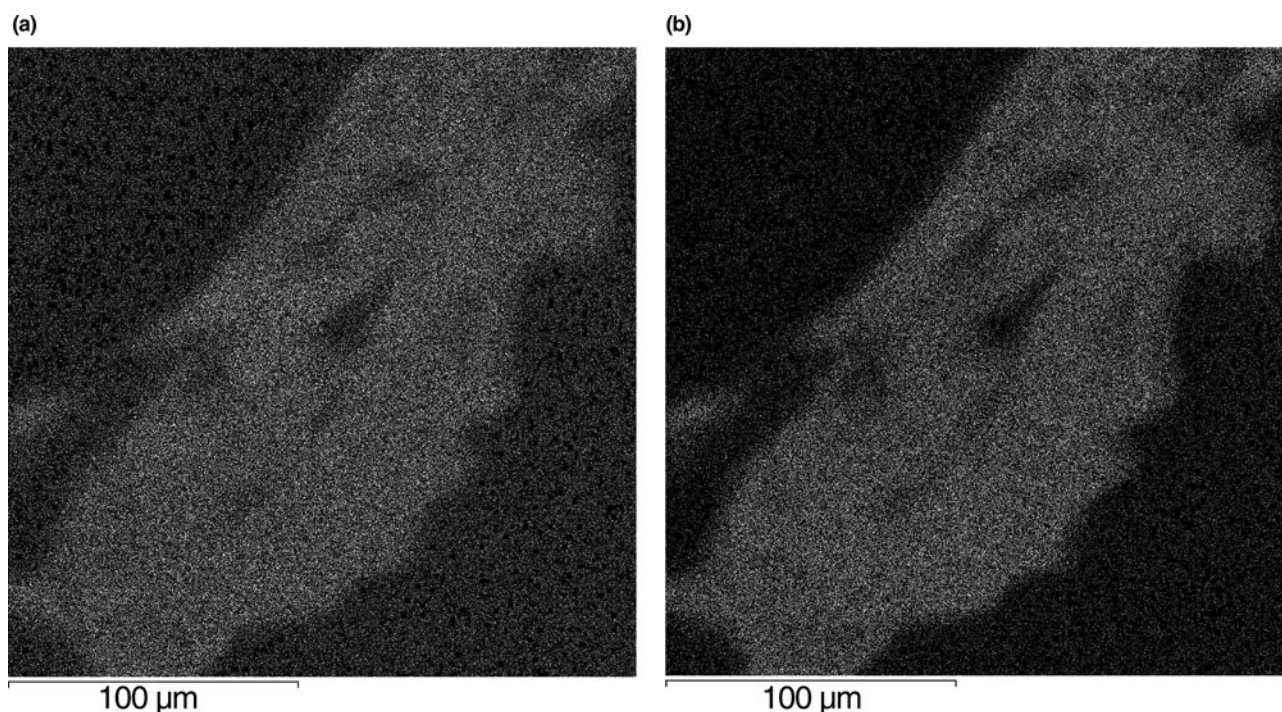


Fig. 10. Images of a sapozhnikovite grain in characteristic X-ray radiation of (a) sulfur and (b) chlorine. Polished section.

Table 2. Chemical composition of sapozhnikovite.

Constituent	Wt.%	Range	S.D.	Standard
Na <sub>2</sub> O	25.05	23.95–25.73	0.49	Albite
Al <sub>2</sub> O <sub>3</sub>	32.44	31.87–32.82	0.35	Albite
SiO <sub>2</sub>	37.58	36.88–38.22	0.43	SiO <sub>2</sub>
HS	4.33*	4.07–4.53	0.16	FeS <sub>2</sub>
Cl	2.22	2.03–2.41	0.13	Scapolite
H <sub>2</sub> O	0.30*			
–O≡(Cl,HS)	–1.55			
Total	100.37			

\*Hydrogen determined as 1.36 wt.% H<sub>2</sub>O was apportioned between HS<sup>–</sup> and H<sub>2</sub>O based on the sulfur content determined by electron microprobe. S.D. – standard deviation.

The crystal structure of sapozhnikovite (Fig. 11) was refined to  $R_1 = 0.0162$  for 334 unique reflections with  $I > 2\sigma(I)$  in the frame of the space group  $P43n$ . Twinning by merohedry Class I (Nespolo and Ferraris, 2000) with an inversion centre as a twinning operator was found in the crystal studied. The atom coordinates, displacement parameters and site occupancies are presented in Table 4. Selected interatomic distances are given in Table 5. The crystallographic information file has been deposited with the Principal Editor of *Mineralogical Magazine* and is available as Supplementary material (see below).

Sapozhnikovite is isostructural to sodalite. In sodalite, extra-framework components (sodium cations and chloride anions) form a  $[\text{Na}_4\text{Cl}]^{3+}$  cluster, which is a distorted tetrahedron. A similar  $[\text{Na}_4(\text{HS})]^{3+}$  cluster occurs in sapozhnikovite.

Sodalite and sapozhnikovite differ distinctly from sulfate-bearing sodalite-group minerals by lower values of the unit-cell parameter  $a$  (below 9.0 Å and above 9.0 Å, respectively) and, respectively, unit-cell volume (see Table 6) that is caused by difference in size between  $\text{SO}_4^{2-}$  and oxygen-free anions.

Table 3. Powder X-ray diffraction data ( $d$  in Å) of sapozhnikovite.

$l_{\text{obs}}$	$d_{\text{obs}}$	$l_{\text{calc}}^*$	$d_{\text{calc}}^{**}$	$h k l$
<b>37</b>	<b>6.30</b>	<b>42</b>	<b>6.304</b>	<b>110</b>
5	4.456	5	4.457	200
1	3.986	1	3.987	210
<b>100</b>	<b>3.638</b>	<b>100</b>	<b>3.639</b>	<b>211</b>
<b>14</b>	<b>2.821</b>	<b>10</b>	<b>2.819</b>	<b>310</b>
<b>18</b>	<b>2.572</b>	<b>21</b>	<b>2.573</b>	<b>222</b>
<b>16</b>	<b>2.382</b>	<b>19</b>	<b>2.383</b>	<b>321</b>
2	2.229	2	2.229	400
<b>29</b>	<b>2.101</b>	<b>33</b>	<b>2.101</b>	<b>411</b>
3	1.993	4	1.993	420
4	1.901	4	1.901	332
4	1.819	3	1.820	422
4	1.748	4	1.748	510
3	1.628	3	1.628	521
8	1.576	11	1.576	440
5	1.529	7	1.529	433
8	1.486	11	1.486	600
8	1.447	12	1.446	611
1	1.410	1	1.410	620
3	1.376	4	1.376	541
3	1.344	5	1.344	622
4	1.315	5	1.314	631
3	1.288	4	1.287	444
1	1.237	1	1.236	640
7	1.214	12	1.213	633
1	1.192	1	1.191	642

The strongest peaks are given in bold

\*For the calculated pattern, only reflections with intensities  $\geq 1$  are given

\*\*For the unit-cell parameters calculated from single-crystal data

## Discussion

The narrow bands at 12,400, 13,400, and 17,300  $\text{cm}^{-1}$  in the absorption spectrum (Fig. 7) are due to the  $^4I_{9/2} \rightarrow ^4F_{5/2}$ ;  $^4I_{9/2} \rightarrow ^4F_{7/2}$  and  $^4I_{9/2} \rightarrow ^4G_{5/2}$  transitions in  $\text{Nd}^{3+}$  ions (Lin *et al.*, 2014).

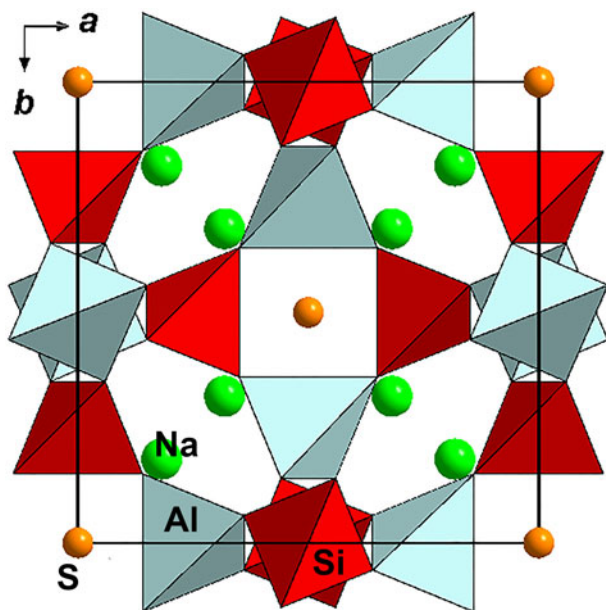


**Fig. 11.** The crystal structure of sapozhnikovite. Hydrogen atoms are not shown. The unit cell is outlined.

The observed photoluminescence with a maximum at  $16,000\text{ cm}^{-1}$  (Fig. 8) corresponds to the  $S_2^{\bullet-}$  radical anion ("•" denotes unpaired electron). The vibration frequency of  $S_2^{\bullet-}$  in sapozhnikovite determined from the distance between vibrational satellites is equal to  $536\text{ cm}^{-1}$ . In luminescence spectra of admixed  $S_2^{\bullet-}$  in alkali halides, maxima in the range of  $16,900\text{--}17,200\text{ cm}^{-1}$  are observed, and vibration frequency at  $\sim 635\text{--}655\text{ cm}^{-1}$  (Kirk *et al.*, 1965). In h aüyne,  $S_2^{\bullet-}$  photoluminescence has a maximum at  $\sim 15,600\text{ cm}^{-1}$  and the vibration frequency of  $S_2^{\bullet-}$  is  $\sim 590\text{ cm}^{-1}$  (Chukanov *et al.*, 2020b). In sulfur-doped sodalites,  $S_2^{\bullet-}$  photoluminescence has a maximum at  $\sim 15,800\text{ cm}^{-1}$  and vibration frequency is equal to  $560\text{ cm}^{-1}$  (Sidike, 2007). In hackmanite, the strongest luminescence peak is located at  $16,200\text{ cm}^{-1}$  and the vibration frequency is equal to  $535\text{ cm}^{-1}$  (Radomskaya, 2021).

The broad band in the range of  $23,000\text{--}28,000\text{ cm}^{-1}$  in the excitation spectrum (Fig. 9) and the shoulder in the absorption spectrum observed in the same spectral region (Fig. 7) are attributed to the  $\pi_u \rightarrow \pi_g^*$  transitions in  $S_2^{\bullet-}$ . The narrow bands with the maxima at  $\sim 30,200$ ,  $\sim 35,000$ , and  $\sim 36,700\text{ cm}^{-1}$  are due to the transitions from the  ${}^6S_{7/2}$  level to  ${}^6P_J$ ,  ${}^6I_J$ , and  ${}^6D_J$  in  $Gd^{3+}$ , respectively (Pankratova *et al.*, 2020).  $Gd^{3+}$  and  $Nd^{3+}$  ions may be located in sodalite cages.

The ESR signal with  $g = 1.99$  could be attributed to  $Gd^{3+}$ . Iton and Turkevich (1977) observed a signal with the same  $g$ -factor in ESR spectra of non-orientated and polycrystalline samples of some hydrated zeolites. On the other hand, the ESR spectrum could be due to the axial  $Fe^{3+}$  centres. A similar broad signal has been observed in beryl (Lin *et al.*, 2013). Nevertheless, both axial  $Fe^{3+}$  and  $Gd^{3+}$  ions should present at sufficiently high abundances to result in significant dipole interaction that induced line broadening. The large amounts of  $Fe^{3+}$  or  $Gd^{3+}$  ions should be detected in the optical absorption spectrum, however no bands corresponding to  $Fe^{3+}$  or  $Gd^{3+}$  were found. Only traces of  $Gd^{3+}$  are displayed in the photoluminescence excitation spectrum (Fig. 9). Therefore, the origin of this signal remains unclear.

The very weak signal with  $g = 2.008$  has been linked to the  $S_2^{\bullet-}$  radical anion by Kowalak *et al.* (2007). Analogous signals of

**Table 4.** Coordinates, equivalent displacement parameters ( $U_{eq}$ , in  $\text{Å}^2$ ) of atoms and site occupancy factors (s.o.f.) in the structure of sapozhnikovite.

Site	x	y	z	$U_{eq}$	s.o.f. or refined number of electrons
Na	0.18168(9)	0.18168(9)	0.18168(9)	0.0202(4)	$Na_{0.977(6)}$
Si	0.25	0.5	0.0	0.00721(17)	$Si_{1.00}$
Al	0.25	0	0.5	0.00705(18)	$Al_{1.00}$
O1	0.13998(11)	0.14994(11)	0.44087(14)	0.0123(2)	$O_{1.00}$
S*	0	0	0	0.0317(6)	$15.50\text{ e}^-$

\*The occupancy of the S site was refined as S vs. O. Based on chemical data, the refined site occupancy of  $S_{0.94(2)}O_{0.06(2)}$  with the number of electrons of 15.50 corresponds to the real occupancy of  $(HS)_{0.61}Cl_{0.30}(H_2O)_{0.08}$ . Excessive water (0.08  $H_2O$  molecules per formula unit; see Table 1) is attributed to the Na site.

**Table 5.** Selected interatomic distances ( $\text{Å}$ ) in the structure of sapozhnikovite.

Si–O1	$1.6220(7) \times 4$	Na–O1	$2.3573(14) \times 3$
Al–O1	$1.7397(7) \times 4$	Na–S	$2.8053(14)$

$S_2^{\bullet-}$  have also been observed in the ESR spectra of other sodalite-group minerals (Chukanov *et al.*, 2020b) and ultramarine analogues prepared from zeolites (Kowalak *et al.*, 2007). However,  $S_2^{\bullet-}$  spectra can be undetectably broadened by radical dynamics and should be very environmentally dependent due to the varying interaction between split  $\pi^*$  states of  $S_2^{\bullet-}$  in different local environments (Rejmak, 2018). In alkali halides  $S_2^{\bullet-}$  radicals have been well-studied and  $g$  components demonstrate strong anisotropy and variability (Vannotti and Morton, 1967; Callens *et al.*, 1989). In ultramarine, the components of the  $g$ -tensor of  $S_2^{\bullet-}$  [ $g_1 = 2.69(6)$ ,  $g_2 = 2.03(4)$  and  $g_3 = 1.86(4)$ ] are quite different from the  $g$ -factor of a free electron (Raulin *et al.*, 2011). Therefore, this signal is tentatively assigned to the  $(SO_3)^{\bullet-}$  radical anion, which, in the ESR spectra of anhydrite and gypsum, shows nearly isotropic signals with  $g = 2.003\text{--}2.004$  (Ryabov *et al.*, 1983; Kasuya *et al.*, 1991). The  ${}^{33}S$  hyperfine structures are difficult to detect for sapozhnikovite due to the very low abundance of the  ${}^{33}S$  isotope and low intensity of the ESR signal.

Another weak signal with  $g = 2.001$  could be assigned either to an anionic vacancy (Vassilikou-Dova and Lehmann, 1990) or to the  $S^{\bullet-}/H_2S^{\bullet-}$  centres (Hausmann, 1966; Symons, 1999). The latter assignment seems more probable taking into account the fact that the intensity of this signal was enhanced by light irradiation from a low-pressure mercury lamp with a wavelength of 185 nm. The  $2HS^{\bullet-} \rightarrow S^{\bullet-} + H_2S^{\bullet-}$  transformation under the exposure of vacuum UV radiation has been reported by Fischer and Gr undig (1965). A similar transformation could occur in sapozhnikovite when exposed to background radiation.

According to the luminescence data, sapozhnikovite contains trace amounts of the  $S_2^{\bullet-}$  radical anion, however, the ESR signal of  $S_2^{\bullet-}$  in sapozhnikovite was not detected, which indicates a very low amount of  $S_2^{\bullet-}$  in the sample studied. Comparisons of the intensity of the signal with h aüyne showed that the content of  $S_2^{\bullet-}$  in sapozhnikovite does not exceed 0.006 wt.%. Such a low content of  $S_2^{\bullet-}$  cannot be detected by means of X-ray structural analysis, but the fact that  $S_2^{\bullet-}$  is likely to be present in sapozhnikovite is important to understand the nature of the observed orange-red luminescence under exposure of UV radiation. We assume that a minor amount of  $S_2^{\bullet-}$  may occur at the S site.

Hypothetically, anionic and neutral extra-framework components occurring in minerals belonging to the sodalite and cancrinite groups, could be used as important geochemical markers as



**Table 6.** Comparative data for sapozhnikovite and related sodalite-group minerals with the  $[Al_6Si_6O_{24}]$  framework having cubic symmetry and the **SOD**-type topology.

Mineral	Sapozhnikovite	Sodalite	Nosean	Haüyne	Lazurite
Formula	$Na_8(Al_6Si_6O_{24})(HS)_2$	$Na_8(Al_6Si_6O_{24})Cl_2$	$Na_8(Al_6Si_6O_{24})(SO_4) \cdot H_2O$	$Na_6Ca_2(Al_6Si_6O_{24})(SO_4)_2$	$Na_7Ca(Al_6Si_6O_{24})(SO_4)S_3^- \cdot H_2O^*$
Crystal system	Cubic	Cubic	Cubic	Cubic	Cubic
Space group	$P\bar{4}3n$	$P\bar{4}3n$	$P\bar{4}3n$	$P\bar{4}3n$	$P\bar{4}3n$
$a$ (Å)	8.9146	8.87–8.88	9.05–9.08	9.08–9.13	9.071–9.09
$V$ (Å <sup>3</sup> )	708.45	697.9–700.7	741–749.6	748.6–761.0	746.4–750.3
Z	1	1	1	1	1
Strong lines of the powder X-ray diffraction pattern:	6.30 (37) 3.638 (100) 2.821 (14) 2.572 (18)	6.28 (34) 3.629 (100) 2.808 (10) 2.562 (18)	9.127 (10) 6.464 (36) 3.718 (100) 2.876 (24)	6.47 (16) 3.72 (100) 2.873 (14) 2.623 (25)	6.437 (18) 4.548 (8) 3.711 (100) 2.875 (16)
$d$ , Å ( $I$ , %)	2.382 (16) 2.101 (29)	2.373 (21) 2.092 (34) 1.569 (16)	2.625 (49) 2.143 (25) 1.607 (11)	2.428 (8) 2.141 (14) 1.781 (10)	2.623 (30) 2.142 (16) 1.782 (9)
Optical data	Isotropic $n = 1.499$	Isotropic $n = 1.483$ – $1.487$	Isotropic $n = 1.461$ – $1.495$	Isotropic $n = 1.494$ – $1.509$	Isotropic $n = 1.502$ – $1.522$
Density (g·cm <sup>-3</sup> )	2.25 (meas.) 2.247 (calc.)	2.27–2.33 (meas.) 2.31 (calc.)	2.25–2.40 (meas.) 2.21 (calc.)	2.44–2.50 (meas.)	2.38–2.45 (meas.) 2.39–2.42 (calc.)
Sources	This proposal	Deer <i>et al.</i> (1963); Peterson (1983); Hassan and Grundy (1984); Bokiý and Borutskiy (2003).	Deer <i>et al.</i> (1963); Taylor (1967); Hassan and Grundy (1989); Bokiý and Borutskiy (2003).	Deer <i>et al.</i> (1963); Löhn and Schulz (1968); Burrigato <i>et al.</i> (1982); Kuribayashi <i>et al.</i> (2018).	Deer <i>et al.</i> (1963); Hogarth and Griffin (1976); Sapozhnikov (1990); Bokiý and Borutskiy (2003); Chukanov <i>et al.</i> (2020b); Sapozhnikov <i>et al.</i> (2021).

\*The revised formula of lazurite was approved by the IMA CNMNC in 2021 (nomenclature proposal 20-H, Miyawaki *et al.*, 2021).

indicators of oxygen, fluorine and sulfur dioxide fugacities (Tauson et al., 2011, 2012; Chukanov et al., 2020a, 2020b).

Sapozhnikovite is probably a late-stage magmatic mineral. The oxalate-bearing cancrinite-group mineral kyanoxalite  $\text{Na}_7(\text{Al}_{5-6}\text{Si}_{6-7}\text{O}_{24})(\text{C}_2\text{O}_4)_{0.5-1.0}\cdot 5\text{H}_2\text{O}$  occurring in close association with sapozhnikovite is an important marker of reductive crystallisation conditions (Chukanov et al., 2010), which resulted in the formation of sapozhnikovite rather than nosean,  $\text{Na}_8(\text{Al}_6\text{Si}_6\text{O}_{24})(\text{SO}_4)\cdot \text{H}_2\text{O}$  – a significant component of some peralkaline rocks of the Lovozero massif. Kyanoxalite is the youngest feldspathoid in this rock; it occurs, together with natrolite, in interstices between crystals of nepheline, sapozhnikovite and aegirine, and replaces peripheral zones of sapozhnikovite grains (Fig. 3).

It is noteworthy that the formation of significant segregations of bituminous matter in peralkaline pegmatites is predated, as a rule, by mass crystallisation of aegirine  $\text{NaFe}^{3+}\text{Si}_2\text{O}_6$  up to the appearance of almost pure aegirine zones in pegmatitic bodies. It is assumed (Ermolaeva et al., 2009) that crystallisation of aegirine could be accompanied by the following redox reactions:  $\text{Na}_2\text{O} + 2\text{FeO} + 4\text{SiO}_2 + \text{CO}_2 \rightarrow 2\text{NaFeSi}_2\text{O}_6 + \text{CO}$ ;  $\text{Na}_2\text{O} + 2\text{FeO} + 4\text{SiO}_2 + 0.5\text{CO}_2 \rightarrow 2\text{NaFeSi}_2\text{O}_6 + 0.5\text{C}$  where C is carbon with the oxidation degree of 0. Similar reactions could lead to the formation of reduced forms of sulfur including the  $\text{HS}^-$  anion.

**Acknowledgements.** The authors are grateful to Peter Leverett, Yuanming Pan, Charles A. Geiger and anonymous referees for the useful discussion. This work was carried-out in accordance with the state task of Russian Federation, state registration number AAAA-A19-119092390076-7. The authors thank the X-ray Diffraction Centre of Saint-Petersburg State University for instrumental and computational resources. The UV/Vis/NIR and photoluminescence spectroscopy was carried out using facilities of the Center for Isotopic-Geochemical Investigations at the Vinogradov Institute of Geochemistry SB RAS. Roman Shendrik has received funding from the Grant of the INRTU Council (15-RAS-2020). IR and Raman spectroscopy investigations were supported by the Russian Science Foundation, grant No. 19-17-00050.

**Supplementary material.** To view supplementary material for this article, please visit <https://doi.org/10.1180/mgm.2021.94>

## References

- Bokiy G.B. and Borutskiy B.E. (editors) (2003) *Minerals. Vol. 2: Framework Silicates*. Moscow, Nauka, 379 pp. [in Russian].
- Bonaccorsi E. and Merlino S. (2005) Modular microporous minerals: cancrinite-davine group and C-S-H Phases. Pp. 241–290 in: *Micro- and Mesoporous Mineral Phases* (G. Ferraris and S. Merlino, editors). Reviews in Mineralogy and Geochemistry, 57. Mineralogical Society of America and the Geochemical Society, Chantilly, Virginia, USA.
- Bragin J., Diem M., Guthals D., Chang S. (1977) The vibrational spectrum and lattice dynamics of polycrystalline ammonium hydrosulfide. *Journal of Chemical Physics*, 67, 1247–1256. <https://doi.org/10.1063/1.434936>
- Britvin S.N., Dolivo-Dobrovolsky D.V. and Krzhizhanovskaya M.G. (2017) Software for processing the X-ray powder diffraction data obtained from the curved image plate detector of Rigaku RAXIS Rapid II diffractometer. *Zapiski Rossiiskogo Mineralogicheskogo Obshchestva (Proc. Russ. Mineral. Soc.)*, 146, 104–107 [in Russian].
- Burrigato F., Maras A. and Rossi A. (1982) The sodalite group minerals in the volcanic areas of Latium. *Neues Jahrbuch für Mineralogie Monatshefte*, 433–445.
- Callens F., Maes F., Matthys P. and Boesman E. (1989)  $^{33}\text{S}$  splittings of some sulphur centres in KCl and NaCl. *Journal of Physics: Condensed Matter*, 1, 6921–6928. <https://doi.org/10.1088/0953-8984/1/39/002>.
- Chukanov N.V. (2014) *Infrared Spectra of Mineral Species: Extended Library*. Springer-Verlag GmbH, Dordrecht–Heidelberg–New York–London, <https://doi.org/10.1007/978-94-007-7128-4>.
- Chukanov N.V. and Chervonnyi A.D. (2016) *Infrared Spectroscopy of Minerals and Related Compounds*. Springer, Cham–Heidelberg–Dordrecht–New York–London, <https://doi.org/10.1007/978-3-319-25349-7>.
- Chukanov N.V., Pekov I.V., Olysykh L.V., Massa W., Yakubovich O.V., Zadov A.E., Rastsvetaeva R.K. and Viginina M.F. (2010) Kyanoxalite, a new cancrinite-group mineral species with extraframework oxalate anion from the Lovozero alkaline pluton, Kola peninsula. *Geology of Ore Deposits*, 52, 778–790.
- Chukanov N.V., Viginina M.F., Zubkova N.V., Pekov I.V., Schäfer C., Kasatkin A.V., Yapaskurt V.O. and Pushcharovsky D.Yu. (2020a) Extra-framework content in sodalite-group minerals: Complexity and new aspects of its study using infrared and Raman spectroscopy. *Minerals*, 10, 363. <https://doi.org/10.3390/min10040363>
- Chukanov N.V., Sapozhnikov A.N., Shendrik R.Yu., Viginina M.F. and Steudel R. (2020b) Spectroscopic and crystal-chemical features of sodalite-group minerals from gem lazurite deposits. *Minerals*, 10, 1042. <https://doi.org/10.3390/min10111042>
- Chukanov N.V., Aksenov S.M. and Rastsvetaeva R.K. (2021a) Structural chemistry, IR spectroscopy, properties, and genesis of natural and synthetic microporous cancrinite- and sodalite-related materials: a review. *Microporous and Mesoporous Materials*, 323, article No. 111098. <https://doi.org/10.1016/j.micromeso.2021.111098>
- Chukanov N.V., Zubkova N.V., Pekov I.V., Shendrik R.Y., Varlamov D.A., Viginina M.F., Belakovskiy D.I., Britvin S.N., Yapaskurt V.O. and Pushcharovsky D.Y. (2021b) Sapozhnikovite, IMA 2021-030. CNMNC Newsletter 62. *Mineralogical Magazine*, 85. <https://doi.org/10.1180/mgm.2021.62>
- Deer W.A., Howie R.A. and Zussman J. (1963) *Rock-forming Minerals. Vol. 4: Framework Silicates*. 1<sup>st</sup> Edition. Longmans, London, pp. 289–302.
- Ermolaeva V.N., Chukanov N.V., Pekov I.V. and Kogarko L.N. (2009) The geochemical and genetic role of organic substances in postmagmatic derivatives of alkaline plutons. *Geology of Ore Deposits*, 51, 513–524.
- Fischer F. and Gründig H. (1965) Optische Absorption und photochemisches Verhalten von  $\text{SH}^-$ ,  $\text{S}^-$  und  $\text{S}^{2-}$ -Zentren in KCl-Kristallen. *Zeitschrift für Physik*, 184, 299–309. <https://doi.org/10.1007/BF01383826>
- Hassan I. and Grundy H.D. (1984) The crystal structures of sodalite-group minerals. *Acta Crystallographica*, 40, 6–13.
- Hassan I. and Grundy H.D. (1989) The structure of nosean, ideally  $\text{Na}_8[\text{Al}_6\text{Si}_6\text{O}_{24}]\text{SO}_4\cdot \text{H}_2\text{O}$ . *The Canadian Mineralogist*, 27, 165–172.
- Hausmann A. (1966) Elektronenspin-Resonanz in Alkalihalogenid-Kristallen mit Schwefel- und Selenzusätzen. *Zeitschrift für Physik*, 192, 313–328.
- Hettmann K., Wenzel T., Marks M. and Markl G. (2012) The sulfur speciation in S-bearing minerals: New constraints by a combination of electron microprobe analysis and DFT calculations with special reference to sodalite-group minerals. *American Mineralogist*, 97, 1653–1661. <http://dx.doi.org/10.2138/am.2012.4031>
- Hogarth D.D. and Griffin W.L. (1976) New data on lazurite. *Lithos*, 9, 39–54.
- Iton L.E. and Turkevich J. (1977) Electron paramagnetic resonance of rare earth ions in zeolites. *Journal of Physical Chemistry*, 81, 435–449. <https://doi.org/10.1021/j100520a015>.
- Kasuya M., Brumby S. and Chappell J. (1991) ESR signals from natural gypsum single crystals: implications for ESR dating. *International Journal of Radiation Applications and Instrumentation. Part D. Nuclear Tracks and Radiation Measurements*, 18, 329–333. [https://doi.org/10.1016/1359-0189\(91\)90027-F](https://doi.org/10.1016/1359-0189(91)90027-F)
- Kirk R.D., Schulman J.H. and Rosenstock H.B. (1965) Structure in the luminescence emission of the  $\text{S}_2^-$  ion. *Solid State Communications*, 3, 235–239.
- Kowalak S., Jankowska A., Zeidler S. and Wieckowski A.B. (2007) Sulfur radicals embedded in various cages of ultramarine analogs prepared from zeolites. *Journal of Solid State Chemistry*, 180, 1119–1124. <https://doi.org/10.1016/j.jssc.2007.01.004>.
- Kuribayashi T., Aoki S. and Nagase T. (2018) Thermal behavior of modulated haiyne from Eifel, Germany: In situ high-temperature single-crystal X-ray diffraction study. *Journal of Mineralogical and Petrological Sciences*, 113, 51–55.
- Lin J., Chen N., Huang D. and Pan Y. (2013) Iron pairs in beryl: New insights from electron paramagnetic resonance, synchrotron X-ray absorption spectroscopy, and *ab initio* calculations. *American Mineralogist*, 98, 1745–1753. <https://doi.org/10.2138/am.2013.4472>.

- Lin H., Chu Rong Gui S., Imakita K. and Fujii M. (2014) Enhanced near infrared emission from the partially vitrified  $\text{Nd}^{3+}$  and silver co-doped zeolite Y. *Journal of Applied Physics*, **115**, 033507, <https://doi.org/10.1063/1.4862232>.
- Löhn J. and Schulz H. (1968) Strukturverfeinerung am gestörten Haiün,  $(\text{Na}_2\text{K}_1\text{Ca}_2)\text{Al}_6\text{Si}_6\text{O}_{24}(\text{SO}_4)_{1.5}$ . *Neues Jahrbuch für Mineralogie, Abhandlungen*, **109**, 201–210 [in German].
- Miyawaki R., Hatert F., Pasero M. and Mills S.J. (2021) Newsletter 60. *Mineralogical Magazine*, **85**, 454–458.
- Nakamoto K. (2008) *Infrared and Raman Spectra of Inorganic and Coordination Compounds, Theory and Applications in Inorganic Chemistry*. John Wiley and Sons, New York.
- Nakamoto K. (2009) *Infrared and Raman Spectra of Inorganic and Coordination Compounds, Part B, Applications in Coordination, Organometallic, and Bioinorganic Chemistry*. John Wiley and Sons, Hoboken.
- Nespolo M. and Ferraris G. (2000) Twinning by syngonic and metric merohedry. Analysis, classification and effects on the diffraction pattern. *Zeitschrift für Kristallographie*, **215**, 77–81.
- Pankratova V., Kozlova A.P., Buzanov O.A., Chernenko K., Shendrik R., Sarakovskis A. and Pankratov V. (2020) Time-resolved luminescence and excitation spectroscopy of co-doped  $\text{Gd}_3\text{Ga}_3\text{Al}_2\text{O}_{12}$  scintillating crystals. *Scientific Reports*, **10**, 20388, <https://doi.org/10.1038/s41598-020-77451-x>.
- Peterson R.C. (1983) The structure of hackmanite, a variety of sodalite, from Mont St-Hilaire, Quebec. *The Canadian Mineralogist*, **21**, 549–552.
- Radomskaya T.A., Kaneva E.V., Shendrik R.Yu., Suvorova L.F. and Vladykin N.V. (2021) Sulfur-bearing sodalite, hackmanite, in alkaline pegmatites of the Inagli massif (Aldan Shield): Crystal chemical features, photochromism, and luminescence. *Geology of Ore Deposits*, **63**(7), 1–9, <https://doi.org/10.1134/S1075701521070060>.
- Raulin K., Gobeltz N., Vezin H., Touat, N., Ledé B. and Moissette A. (2011) Identification of the EPR signal of  $\text{S}_2^-$  in green ultramarine pigments. *Physical Chemistry Chemical Physics*, **13**(20), 9253–9259, <https://doi.org/10.1039/C0CP02970J>.
- Rejmak P. (2018) Structural, optical, and magnetic properties of ultramarine pigments: A DFT insight. *The Journal of Physical Chemistry C*, **122**(51), 29338–29349, <https://doi.org/10.1021/acs.jpcc.8b09856>.
- Rigaku Oxford Diffraction (2018) *CrysAlisPro Software System, v. 1.171.39.46*, Rigaku Corporation, Oxford, UK.
- Ryabov I.D., Bershov L.V., Speranskiy A.V. and Ganeev I.G. (1983) Electron paramagnetic resonance of  $\text{PO}_3^{3-}$  and  $\text{SO}_3^-$  radicals in anhydrite, celestite and barite: the hyperfine structure and dynamics. *Physics and Chemistry of Minerals*, **10**(1), 21–26, <https://doi.org/10.1007/BF01204322>.
- Sapozhnikov A.N. (1990) Indexing of additional reflections on the X-ray Debye diffraction patterns of lazurite concerning the study of modulation of its structure. *Zapiski Vsesoyuznogo Mineralogicheskogo Obshchestva (Proceedings of the Soviet Mineralogical Society)*, **119**(1), 110–116 [in Russian].
- Sapozhnikov A.N., Tauson V.L., Lipko S.V., Shendrik R.Yu., Levitskii V.I., Suvorova L.F., Chukanov N.V. and Vigasina M.F. (2021) On the crystal chemistry of sulfur-rich lazurite, ideally  $\text{Na}_7\text{Ca}(\text{Al}_6\text{Si}_6\text{O}_{24})(\text{SO}_4)(\text{S}_3)^- \cdot n\text{H}_2\text{O}$ . *American Mineralogist*, **106**, <https://doi.org/10.2138/am-2020-7317>.
- Sheldrick G.M. (2015) Crystal structure refinement with SHELXL. *Acta Crystallographica*, **C71**, 3–8.
- Sheppard N. (1949) The assignment of the vibrational spectra of ethyl mercaptan and the ethyl halides, and the characterization of an SH deformation frequency. *The Journal of Chemical Physics*, **17**, 79–83, <https://doi.org/10.1063/1.1747057>.
- Sidike A., Sawuti A., Wang X.M., Zhu H.J., Kobayashi S., Kusachi I. and Yamashita N. (2007) Fine structure in photoluminescence spectrum of  $\text{S}_2^-$  center in sodalite. *Physics and Chemistry of Minerals*, **34**(7), 477–484, <https://doi.org/10.1007/s00269-007-0161-y>.
- Symons M.C.R. (1999) The radical-cation of hydrogen sulfide. *Physical Chemistry & Chemical Physics*, **1**, 4767–4768, <https://doi.org/10.1039/A906248C>.
- Tauson V.L., Sapozhnikov A.N., Shinkareva S.N. and Lustenberg E.E. (2011) Indicative properties of lazurite as a member of clathrasil mineral family. *Doklady Earth Sciences*, **441**, 1732–1737, <https://doi.org/10.1134/S1028334X11120312>.
- Tauson V.L., Goettlicher J., Sapozhnikov A.N., Mangold S., Shinkareva S.N. and Lustenberg E.E. (2012) Sulphur speciation in lazurite-type minerals  $(\text{Na,Ca})_8[\text{Al}_6\text{Si}_6\text{O}_{24}](\text{SO}_4)_2$  and their annealing products: a comparative XPS and XAS study. *European Journal of Mineralogy*, **24**, 133–152, <https://doi.org/10.1127/0935-1221/2011/0023-2132>.
- Taylor D. (1967) The sodalite group of minerals. *Contributions to Mineralogy and Petrology*, **16**, 172–188.
- Vannotti L.E. and Morton J.R. (1967) Paramagnetic-resonance spectra of  $\text{S}_2^-$  in alkali halides. *Physical Review*, **161**, 282–286, <https://doi.org/10.1103/PhysRev.161.282>.
- Vassilikou-Dova A.B. and Lehmann G.P. (1990) Paramagnetic defects in the mineral haiünite. *Crystal Research & Technology*, **25**, 525–529, <https://doi.org/10.1002/crat.2170250513>.